

TEXTURES OF PARAGNEISSES FROM THE KTB DRILLING SITE, NE BAVARIA (FRG)

F. HEINICKE, H.-G. BROKMEIER and M. DAHMS
GKSS Research Center, Max Planck Str., D-2054 Geesthacht, FRG

H. J. BUNGE
Department of Physical Metallurgy, Technical University Clausthal,
D-3392 Clausthal-Z., FRG

J. PANNETIER and C. RITTER
Institut Laue-Langevin, 156X, F-38042 Grenoble Cédex, France

H. DE WALL
IGDL, Univ. Göttingen, Goldschmidtstr. 3, D-3400 Göttingen, FRG

From September 1987 to April 1989 a pilot boring for the German Continental Deep Drilling Project (KTB) was made about 80 km east of Bayreuth, NE Bavaria (FRG). The final depth of the drill hole was 4000m⁽¹⁾. The drilling site is situated at the western margin of the Bohemian Massif, an area of crystalline rocks which has been deformed frequently during a time span of several hundred millions of years. The rock sequence found in the borehole belongs completely to a geologic nappe (named ZEV), which is thought to have moved to its actual position during a late phase of the variscan deformation (330 Ma ago). Its deformation is significantly distinct from that found in the surrounding 'allochthonous' units⁽²⁾.

The rocks of the ZEV are mostly paragneisses and amphibolites of variable compositions. Several paragneiss samples were chosen for textural investigations from the drilled cores. This contribution is restricted to the texture analysis of one specimen, further results are presented elsewhere^(3,4).

SAMPLE DESCRIPTION

Specimen 71B5b (depth 470m) is subject of the texture analysis presented here. This specimen is typical for the oldest deformation found within the paragneisses. It contains the mineral cyanite which indicates a deformation typical for the ZEV at $P=6-8\text{ kbar}$, $T=650-750^\circ\text{C}$, 390 my ago⁽²⁾. The diaphrotic reactions⁽⁵⁾ which are common in the paragneisses are weakly developed, so most of the biotite and oligoclase is preserved. The mineralogical composition is roughly: quartz (45%), oligoclase (30%), biotite (10%), muscovite, cyanite + sillimanite, garnet.

Some ribbon quartz is developed and there are no recrystallized grains at grain boundaries (in contrast to other specimens). Macroscopically, the sample is dark with some light bands (quartz + oligoclase). The foliation is well developed due to the separation of biotite which is significant especially in the section parallel to the lineation (XZ-section, cf. fig.1).

EXPERIMENTAL

The texture measurements were carried out at ILL, Grenoble, using instrument D1B. The D1B instrument offers an ^3He -filled 80° banana-type detector with an angular resolution of 0.2° . A monochromatic neutron beam with $\lambda=2.5237\text{\AA}$ was produced by a graphite-002 monochromator.

For the measuring procedure a small cylinder (9mm in length, 18mm in diameter) has been prepared from the drill core and mounted on an aluminium pin. The 2θ range covered by the detector was $12-92^\circ$, the corresponding d-space range $1.75-12.1\text{\AA}$. The number of 607 cradle positions were chosen in order to approximate an equal area scan. Additionally 96 cradle positions were used to cover the blind area⁽⁶⁾. The measuring time per point was approx. 120s (total time: 28h, which includes the movement of the cradle).

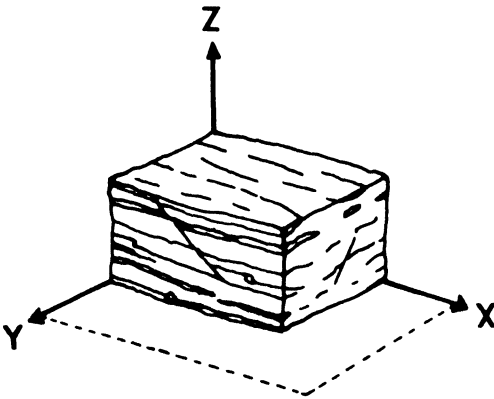


Fig. 1a: Relation between the rock sample and an orthogonal coordinate system: plane XY is parallel to the foliation plane; X is oriented parallel to the macroscopic lineation.

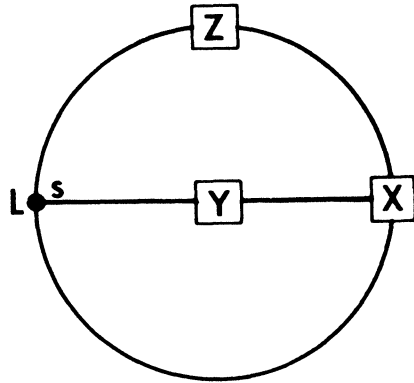


Fig. 1b: Relation between the rock sample and a pole figure using the orthogonal coordinate system.
s: trace of the foliation
L: lineation

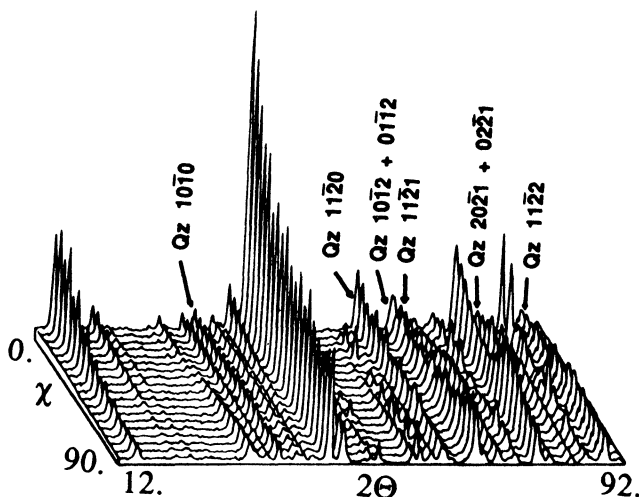


Fig. 2: Stack of diffraction spectra (specimen 71B5b) demonstrating the influence of the texture for $\phi = \text{const}$; $\chi = 0$ is parallel to direction Z, $\chi = 90$ is parallel to direction Y (cf. fig. 1). The quartz peaks used for ODF calculation are indicated.

DATA TREATMENT

The data produced by the D1B equipment consist of 2θ spectra, one spectrum per cradle position. In figure 2 a stack of spectra demonstrates the texture qualitatively (cradle angle $\phi = \text{constant}$). A large number of peaks is present, which is due to the low crystallographic symmetry of oligoclase (tricline) and mica (biotite + muscovite: monocline). The problem of overlapping reflexions is well known. Several peaks belonging to one or a mixture of phases were separated by peak profile analysis⁽⁷⁾. The quartz peaks used for further treatment are indicated in figure 2. Unfortunately, the quartz-(10-11+01-11) peak which is the strongest one in figure 2 cannot be separated from muscovite (006) and is not used.

A pole figure data set is produced from the separated data by calculating pole figure angles β, α from cradle angles ϕ, χ , taking into account the $\omega - \theta$ difference at the specific peak⁽⁶⁾. The view direction of the pole figures is towards the progressive drilling direction.

ODF CALCULATION

The ODF has been calculated using quartz pole figures (10-10), (11-20), (10-12+01-12), (11-21), (20-21+02-21) and (11-22). The purely trigonal Bragg reflections ($|h| \neq |k|$) were divided in accordance to their structure

factors ((10-12):91% vs. (01-12):9% and (20-21):10% vs. (02-21):90%, space group: $P3_121$ (IT)). The complete ODF was calculated using the positivity condition^(8,9). The pole figures (70-72),(16,30,-46,9),(04-43) and (0001) were introduced during this procedure to minimize negative intensity values. The degree of series expansion was $L_{\max}=16$ because the contribution of higher degrees is negligible. The complete ODF is presented in 2σ -sections⁽¹⁰⁾, the data of figure 5 are smoothed by an Gaussian function (12.5°) to accentuate the main structures.

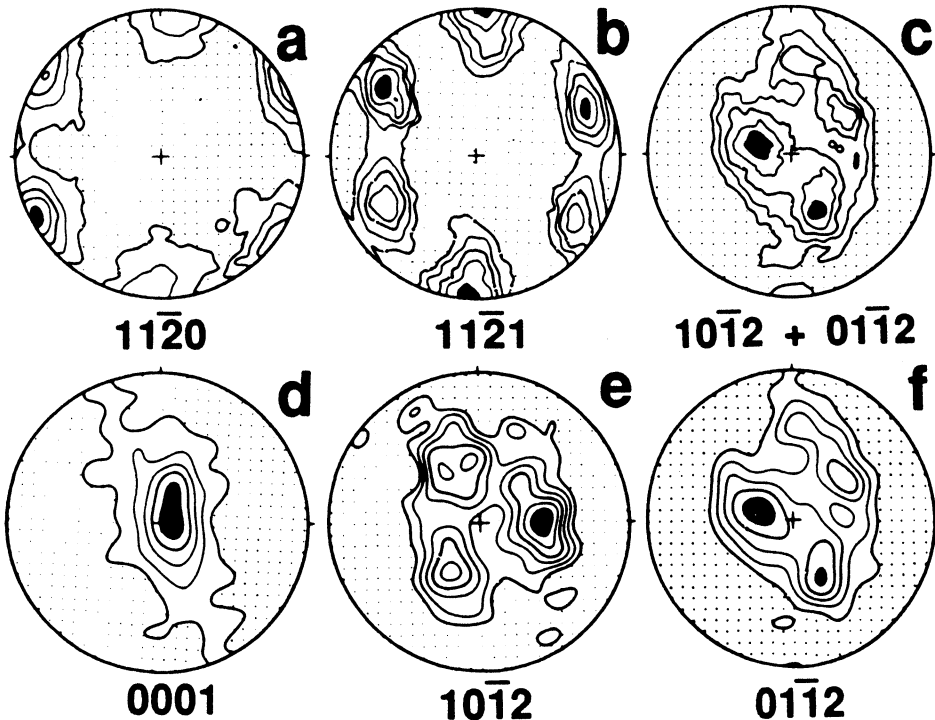


Fig. 3: Pole figures of specimen 71B5b, a-c: measured, d-f: recalculated ($L_{\max}=16$). Lambert Projection, lower hemisphere, all contour labels are multiples of random distribution. (a) min=0.32, max=3.38, steps:1.0, 1.5,...3.0; (b) min=0.40, max=1.91, steps:1.0,1.2,...,1.8; (c) min=0.24, max=2.37, steps:1.0,1.3,...,2.2; (d) min=-0.04, max=5.75, steps: 1.0,2.0,...5.0; (e) min=-0.02, max=2.79, steps: 1.0,1.3,...,2.5; (f) min=0.24, max=2.44, steps: 1.0,1.3,...,2.2; dotted: below 1.; black: above highest contour.

DISCUSSION

The quartz texture of specimen 71B5b is considerably stronger than that of other specimens investigated. This is due to the influence of the ribbon quartz which contributes mainly to the quartz volume and the absence of younger quartz recrystallisation. The texture found produces very simple pictures (figure 3+5) which are close to a single crystal orientation. Nevertheless there is some evidence of girdle distribution

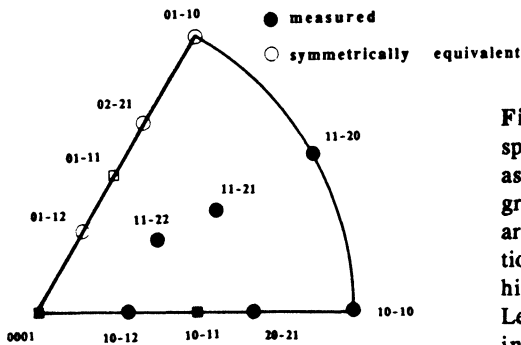
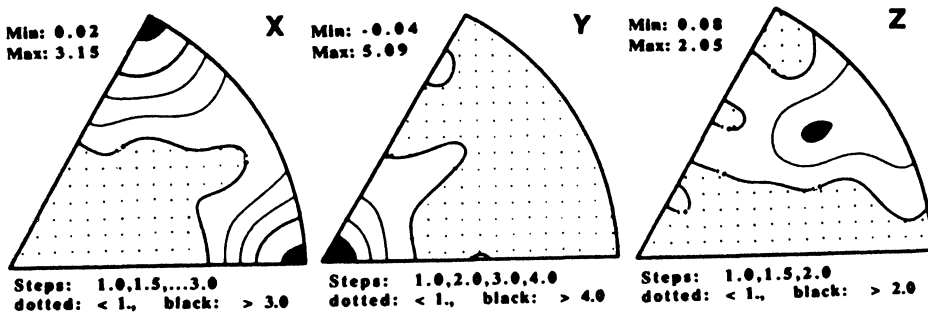


Fig.4: Inverse pole figures, specimen 71B5b. Directions X,Y,Z as indicated in figure 1b. Stereographic projection, contour labels are multiples of random distribution. Dotted: below 1., black: above highest contour. Left: Projection of quartz lattice indices.

which is asymmetric with respect to the external coordinate system, indicating some portion of simple shear. This phenomenon is in accordance with other shear sense criteria (rotated clasts, shear band foliation)(4). The inverse polefigures (figure 4) exhibit the maximum (direction Y) whereas the girdle is not touched by directions X and Z.

The quality of ODF calculation is demonstrated by comparison of measured and recalculated pole figures (figure 3). The asymmetric portion of the texture is reflected by the (11-20) and the (0001) pole figure. The comparison of (11-21) and (10-12+01-12) demonstrates the difference between a 'hexagonal' and a 'trigonal' pole figure. The measured pole figure of (10-12+01-12) is dominated by (01-12) because of its higher structure factor.

In the ODF (figure 5) two elements of the quartz texture are remarkably distinct: the single girdle and the central maximum. This feature may be interpreted as a combination of two deformation types, probably ribbon vs. matrix quartz or older vs. younger grains.

Acknowledgements

Part of this work has been funded by the German Research Foundation (DFG) under contract numbers BR961/1+2 and WE488/24. We are grateful to ILL, Grenoble and GKSS, Geesthacht for access to their facilities, respectively.

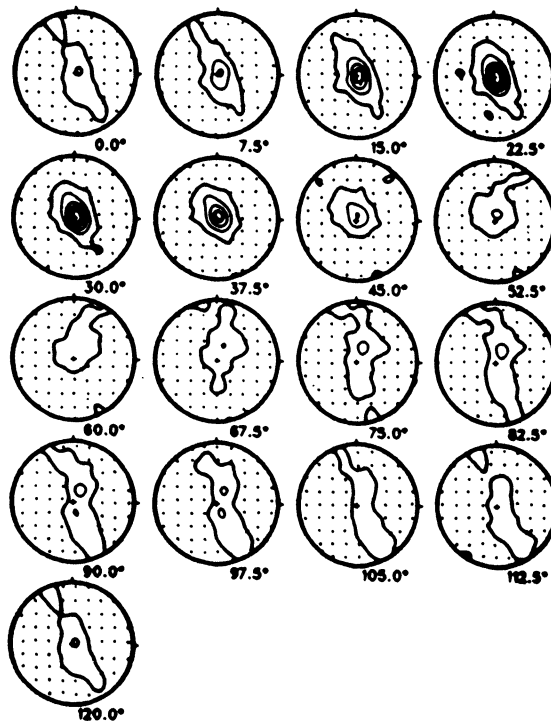


Fig. 5: Complete ODF of specimen 71B5b (2σ -sections). The data have been smoothed by a Gaussian function (12.5°). Stereographic projection. min=-0.08, max=10.41, steps: 1.,3.,5.,7.,9.; dotted: below 1.

REFERENCES

1. R. Emmermann and H. Rischmüller, *GEOWEW* 8,9,241-257 (1990)
2. A. Vollbrecht, K. Weber and J. Schmoll, *Tectonophysics*, 157,123-133 (1989)
3. H.-G. Brokmeier, F. Heinicke, H.J. Bunge and C. Ritter, *KTB REPORT* 89-3,408 (1989)
(The KTB Report is a periodical of the KTB project: KTB project magement, NLFb Hannover, Postfach 510153, D-3000 Hannover 51)
4. F. Heinicke and H. de Wall, *KTB Report* 90-? (in prep.)
5. H. Müller, M. Tapfer, R. Emmermann and W. Wimmenauer, *KTB Report* 89-3,61-66 (1989)
6. H.J. Bunge, H.R. Wenk and J. Pannetier, *Textures and Microstructures*, 5,153-170 (1982)
7. A. Filhol, J.-Y. Blanc, A. Antoniadis and J. Berruer: ABFFit for the Vax (Manual for the version 3.0), ILL 88FI05T, 77 p. (1988)
8. M. Dahms and H.J. Bunge, *Textures and Microstructures*,10,21-35 (1988)
9. M. Dahms and H.J. Bunge, *J. Appl. Cryst.*,22,439-447 (1989)
10. S. Matthies, K. Helmig and K. Kunze, *phys. stat. sol. (b)*,157,71-83 (1990)